Degenerate four-wave mixing in noncentrosymmetric materials

Ivan Biaggio
Institute of Quantum Electronics, Swiss Federal Institute of Technology, ETH Hönggerberg, CH-8093 Zürich, Switzerland
(Received 16 July 2001; published 16 November 2001)

This work treats degenerate four-wave mixing (DFWM) in noncentrosymmetric materials, taking into full account the fact that the DFWM signal arises from third-order nonlinear optical effects as well as from two distinct combinations of second-order effects: second-harmonic generation plus difference frequency generation and optical rectification plus Pockels effect. Because of these second order ''cascaded'' contributions, the DFWM signal becomes dependent on details of the experimental setup that do not normally matter for centrosymmetric materials, such as the wave vectors of the interacting beams and the pulse duration. The origin, consequences, and possible applications of these effects are discussed for both the ''forward'' and the ''phase-conjugation'' DFWM configurations. All second-order contributions are described quantitatively by introducing effective third-order susceptibilities, and their value is discussed using the example of two materials: ferroelectric $KNbO_3$ and the organic salt 4-*N*,*N*-dimethylamino-4′-*N*′-methyl-stilbazolium tosylate.

DOI: 10.1103/PhysRevA.64.063813 PACS number(s): 42.65.An, 42.65.Hw, 78.20.Jq, 42.65.Ky

In noncentrosymmetric materials, the optical electric field can induce a second-order nonlinear polarization that again interacts with the optical field to create a new nonlinear polarization that is then proportional to the third power of the electric field [1–8]. Such a ''cascading'' of second-order processes can contribute to typical third-order nonlinear optical phenomena such as the optical Kerr effect, self-phase modulation, soliton formation, and the interaction of different optical waves [9]. Cascaded contributions are important because they entail a new possibility to optimize nonlinear optical materials for typical third-order applications, and because they lead to a sensitivity to experimental parameters (such as the wave vectors of the interacting optical waves) that are not relevant for pure third-order interactions, thus affecting experiments in unusual ways.

Degenerate four-wave mixing (DFWM) is a commonly used experimental technique for the determination of the third-order nonlinear response. It allows the measurement of most elements of the third-order nonlinear optical susceptibility tensor that describe the interaction of optical fields at a single frequency. Second-order contributions to DFWM are possible via two mechanisms: second-harmonic generation plus difference frequency generation (SHG/DFG) and optical rectification plus linear electro-optic (Pockels) effect (OR/EO). In order to enable a reliable and reproducible determination of third-order nonlinear optical susceptibilities by DFWM, it is necessary to quantitatively predict the relative contributions of each cascaded effect and of the genuine third-order effects in the various possible DFWM experimental setups.

Second-order contributions to nondegenerate wave mixing were first discussed in Ref. [2], where the principles and most important features of the cascading contributions have already been recognized. Second-order contributions to DFWM have been analyzed in Refs. [10–13], and the peculiar geometry dependence of the OR/EO contribution to DFWM was first pointed out in Refs. [10,12]. However, no complete treatment of DFWM that takes into account all second-order contributions has been published to date. An important point that has not been treated consistently in the literature is connected to the question of how the induced second-order polarization interacts with an electric field to generate an effective third-order polarization. It is possible to identify two mechanisms for this to happen: directly through the material polarization, and indirectly through a macroscopic field that is sometimes (but not always) associated with the material polarization. Reference [11] did not include the direct mechanism, which lead to a SHG/DFG contribution too large by a factor of the order of the refractive index squared, and to an incorrect description of the OR/EO contribution. Reference [12] considered both direct and indirect mechanisms, but slightly overestimated the magnitude of the first one, while the contribution from SHG/DFG was neglected. In addition, both Ref. [11] and Ref. [12] considered only the ''phase-conjugation'' DFWM configuration where two of the interacting beams are counterpropagating [14]. Reference [13] expanded on the treatment of Ref. [12] by including piezoelectric effects, took both direct and indirect mechanisms properly into account, and considered also the ''forward'' DFWM configuration, but still limited itself to the OR/EO contributions.

This work presents a general, detailed treatment of DFWM where all second-order contributions are taken into account for the two experimental configurations that come into considerations for bulk materials. The present complete treatment is a prerequisite for a proper analysis of any DFWM experiment performed in noncentrosymmetric materials. It makes it possible to determine correct values for the third-order susceptibilities and to compare results obtained with different experimental setups.

I will first present the nomenclature and formalism used in this work by reviewing the usual treatment of DFWM in a pure third-order material and describing the two experimental geometries with which DFWM can be realized. I will then introduce the two mechanisms with which a nonlinear polarization can interact with the electric field of an optical wave. From this discussion I will then derive expressions for both the SHG/DFG and the OR/EO contributions to DFWM, and define an effective third-order susceptibility tensor that comprises all second- and third-order contributions. Finally, I

will discuss the manifestations of these second-order contributions and their dependence from the experimental parameters in the example of two different materials: the ferroelectric oxide $KNbO_3$ and the molecular crystal 4-*N*,*N*-dimethylamino-4′-*N*′-methyl-stilbazolium tosylate (DAST).

I. GENERAL DESCRIPTION OF DFWM FOR PURE THIRD-ORDER NONLINEARITIES

The following is a short review of DFWM for the case where the interaction of the optical waves is mediated only by a pure third-order effect. It serves as an introduction to the subject of DFWM and to the formalism and the definitions that are used throughout this work.

In the most general case of DFWM there are three separate ''input'' waves that can be distinguished by their propagation direction. We are interested in the case where the interacting beams are weakly focused into the material and can be described by spatially and time-modulated plane waves. Then the total electric field at a position $\vec{r}$ and time t can be written in the form

$$\vec{E}(\vec{r},t)=\frac{1}{2}\{\vec{E}(\omega,\vec{k}_1)\exp[i(\vec{k}_1\vec{r}-\omega t)] + \vec{E}(\omega,\vec{k}_2)\exp[i(\vec{k}_2\vec{r}-\omega t)] + \vec{E}(\omega,\vec{k}_3)\exp[i(\vec{k}_3\vec{r}-\omega t)]+\text{c.c.}\}. \quad (1)$$

This represents three plane waves with the same frequency ω and three different wave vectors $\vec{k}_i$. They are described by complex amplitudes $\vec{E}(\omega,\vec{k}_i)$ that are nearly constant on the time-scale of the optical frequency and the space scale of the optical wave vector. ''+c.c.'' indicates addition of the complex-conjugate term.

In a nonlinear optical material with an instantaneous and local third-order response, the electric field (1) induces a material polarization which, in SI units, can be written as [15,9,16]

$$P_i^{(3)}(\vec{r},t)=\epsilon_0\chi_{ijkl}^{(3)}E_j(\vec{r},t)E_k(\vec{r},t)E_l(\vec{r},t), \quad (2)$$

where the Einstein summation convention over repeated indices is used, and $\chi_{ijkl}^{(3)}$ is the third-order susceptibility tensor in the time domain.

Given the field (1), the material polarization (2) has a complicated time and space-dependence corresponding to a sum of various plane-wave terms with different frequencies and wave vectors. For DFWM one is interested in those terms that have the frequency ω, which are produced by the interaction of all three waves in Eq. (1), and which can radiate a signal wave in a bulk material. By judicious choice of the wave vectors $\vec{k}_1$, $\vec{k}_2$, and $\vec{k}_3$ one can obtain a well-defined signal wave from the one single term with the complex amplitude

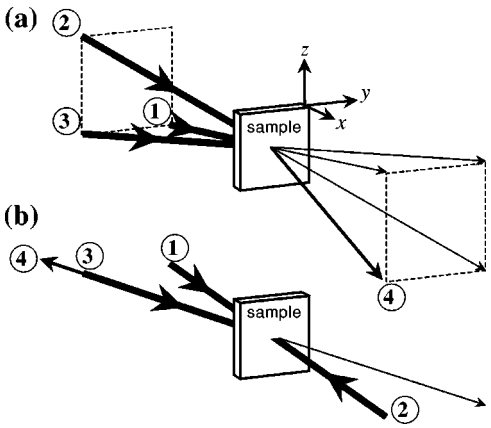

FIG. 1. Two possibilities for an experimental realization of DFWM. (a) ''Forward geometry'': The three input beams 1, 2, and 3 propagate in the same general direction. They go through the vertices of a square in a plane parallel to the surface of the sample and nearly perpendicular to the propagation direction and they meet in the sample. The signal beam 4 exits the sample so that, in the square defined by the three transmitted input beams, it hits the corner opposite to the one of beam 3. (b) ''Phase-conjugation geometry'': Beams 1 and 2 are counterpropagating to each other, and all interacting beams propagate inside the same plane. The signal beam 4 is then counterpropagating to beam 3.

$$P_i^{(3)}(\omega,\vec{k}_4)=\frac{3}{2}\epsilon_0\chi_{ijkl}^{(3)}(-\omega,-\omega,\omega,\omega,-\vec{k}_4,-\vec{k}_3,\vec{k}_2,\vec{k}_1) \times E_j(-\omega,-\vec{k}_3)E_k(\omega,\vec{k}_2)E_l(\omega,\vec{k}_1). \quad (3)$$

where $\vec{k}_4=\vec{k}_1+\vec{k}_2-\vec{k}_3$, $E_j(-\omega,-\vec{k}_3)$ is the complex conjugate of $E_j(\omega,\vec{k}_3)$, and $\chi_{ijkl}^{(3)}(-\omega,-\omega,\omega,\omega,-\vec{k}_4,-\vec{k}_3,\vec{k}_2,\vec{k}_1)$ is the complex third-order susceptibility tensor. Under the assumption that the third order response is both instantaneous and local, it does not depend from either the frequencies or the wave vectors and is a constant directly related to the time-domain tensor introduced in Eq. (2). However, it is often useful to consider some slight noninstantaneous effects that lead to a frequency dispersion. I also explicitly included a wave vector dependence in Eq. (3) because it will be required for the effective third-order susceptibility introduced below to account for the second-order contributions. Only for a pure third-order effect the locality assumption we introduced above removes any wave vector dependence, and the wave vector arguments can be dropped.

There are two alternative experimental setups where a unique signal wave is radiated by the polarization (3). They are sketched in Fig. 1. In both of these configurations the signal wave is emitted in a phase-matched way over the whole thickness of the material [17]. Besides Eq. (3), there are two other polarization components at the frequency ω that have wave vectors $\vec{k}_4=\vec{k}_1-\vec{k}_2+\vec{k}_3$ and $\vec{k}_4=-\vec{k}_1+\vec{k}_2+\vec{k}_3$. However, the magnitude of these wave vectors does not fulfill the dispersion relation of a propagating electromagnetic wave of frequency ω. The corresponding DFWM signal, which has a different propagation direction than the

one radiated by Eq. (3), can only be observed in thin samples [18]. We will not consider this case any further.

The numerical factor of 3/2 in Eq. (3) is a degeneracy factor that arises when substituting Eq. (1) into Eq. (2) and collecting terms with the same space and time dependence to obtain Eq. (3) [19].

The nonlinear polarization (3) gives rise to the signal wave in DFWM by radiating an electric field $\vec{E}^S$ that must fulfill the wave equation

$$\vec{\nabla}\times\vec{\nabla}\times\vec{E}^S(\vec{r},t)=-\frac{1}{c^2}\frac{\partial^2}{\partial t^2}\left[\overleftrightarrow{\epsilon}\vec{E}^S(\vec{r},t)+\frac{1}{\epsilon_0}\vec{P}^{(3)}(\vec{r},t)\right], \tag{4}$$

where c is the speed of light in vacuum and $\vec{P}^{(3)}(\vec{r},t)=(1/2)\vec{P}^{(3)}(\omega,\vec{k}_4)\exp[i(\vec{k}_4\vec{r}-\omega t)]+\text{c.c.}$. The wave vector $\vec{k}_4$ of the polarization (3) has the right magnitude for phase-matched radiation of the field $\vec{E}^S$: for $\vec{P}^{(3)}$ oriented along a main axis i of the dielectric tensor, $k_4=\epsilon_{ii}\omega/c$. In the slowly varying amplitude approximation and as long as the signal wave remains much weaker than the other waves, Eq. (4) implies that $\vec{E}^S$ will grow linearly with propagation distance L as

$$E_i^S(\omega,\vec{k}_4)=L\frac{ik_4}{2\epsilon_0}\epsilon_{ij}^{-1}P_j^{(3)}(\omega,\vec{k}_4), \tag{5}$$

where L is the thickness of material along the wave vector $\vec{k}_4$. Relating the electric fields $E_i^n=E_i(\omega,\vec{k}_n)$ to intensities $I_n=(c\epsilon_0/2)\sqrt{\epsilon_{ii}}|E_i^n|^2$ and using Eq. (3) one obtains, for individual field amplitudes E_j^3, E_k^2, and E_l^1 polarized along the main axes j, k, and l, respectively,

$$I_S=L^2\frac{\omega^2}{c^4\epsilon_0^2}\frac{I_1I_2I_3}{n_in_jn_kn_l}\left|\frac{3}{2}\chi_{ijkl}^{(3)}\right|^2, \tag{6}$$

where n_i is the refractive index for light polarized along i, and $\chi_{ijkl}^{(3)}$ is the third-order susceptibility tensor introduced in Eq. (3) with the frequency and wave vector arguments omitted.

For pulsed experiments it is useful to express the signal energy F_S as a function of the input pulse energies F_n, with all energies measured outside the sample,

$$F_S=\xi L^2\frac{T_iT_jT_kT_l}{n_in_jn_kn_l}F_1F_2F_3|\chi_{ijkl}^{(3)}|^2, \tag{7}$$

where F_n is the pulse energy in beam n and ξ is a factor that is proportional to the spatial and temporal pulse overlap integrals in the material. The ''calibration factor'' ξ must be determined for any DFWM experimental setup in order to be able to measure absolute values for the nonlinear optical susceptibilities. The T_i are the intensity transmission factors for a beam with polarization parallel to the i axis that propagates from outside the sample to the *middle* of the sample. They can be determined experimentally, or they can be calculated from normal Fresnel reflection losses and from the linear absorption constant α_i of the material

$$T_i=\left[1-\left(\frac{n_i-1}{n_i+1}\right)^2\right]\exp(-\alpha_iL/2). \tag{8}$$

Expression (7) is the final result that can be used in any centrosymmetric material to determine experimentally the components of the third-order susceptibility tensor $\chi_{ijkl}^{(3)}$. Note that the results derived here are valid for both DFWM configurations in Fig. 1. The labelling of the beams has been chosen in such a way that Eq. (3) and the discussion surrounding it apply for both configurations.

II. PRINCIPLE AND DESCRIPTION OF CASCADED SECOND-ORDER EFFECTS

We will now review the principles of the cascading process and derive a general expression for the effective third-order polarization it induces. In order not to unnecessarily restrict this particular argument to DFWM, let us consider three plane wave, but otherwise arbitrary, ''input'' electric fields $\vec{E}^i(\vec{r},t)=\vec{E}^i\exp[i(\vec{k}_i\cdot\vec{r}_i-\omega t)]$ with complex amplitudes $\vec{E}^1$, $\vec{E}^2$, and $\vec{E}^3$ $[\vec{E}^i=\vec{E}(\omega_i,\vec{k}_i)]$ and assume that $\vec{E}^1$ and $\vec{E}^2$ combine to generate a second-order polarization $\vec{P}^{(2)}$. This polarization can be described with the same assumptions and formalism used in the preceding section. Its complex amplitude is

$$P_p^{(2)}(\omega_p,\vec{k}_p)=K_1\epsilon_0\chi_{pkl}^{(2)}(-\omega_p,\omega_2,\omega_1)E_k^2E_l^1, \tag{9}$$

where K_1 is the appropriate degeneracy factor. This nonlinear polarization has the space- and time dependence of a plane wave. When discussing DFWM later on, we will consider the special cases where $\omega_p=0$ (optical rectification) or $\vec{k}_p=0$ (a homogenous polarization harmonically modulated in time).

Let us start by establishing the conditions under which a nonlinear polarization with the complex amplitude (9) can induce an electric field $\vec{E}^P$. First, the displacement field

$$D_i^P(\vec{r},t)=\epsilon_0\epsilon_{ij}E_j^P(\vec{r},t)+P_i^{(2)}(\vec{r},t), \tag{10}$$

must be divergence-free in the absence of free charges. Second, for $\omega_p=0$ the curl of the electric field $\vec{E}^P$ must vanish,

$$\vec{\nabla}\times\vec{E}^P(\vec{r})=\vec{0}, \tag{11}$$

while for $\omega_p\neq0$ $\vec{E}^P$ must fulfil the wave equation

$$\vec{\nabla}\times\vec{\nabla}\times\vec{E}^P(\vec{r},t)=-\frac{1}{c^2}\frac{\partial^2}{\partial t^2}\left[\overleftrightarrow{\epsilon}\vec{E}^P(\vec{r},t)+\frac{1}{\epsilon_0}\vec{P}^{(2)}(\vec{r},t)\right]. \tag{12}$$

These conditions lead to separate solutions for oscillatory and static polarizations. For the purposes of this paper, a polarization can be seen as static when its time-modulation period is of the order of the laser-pulse duration.

Consider an oscillating ($\omega_p \neq 0$) nonlinear polarization in a coordinate system where ϵ_{ij} is diagonal. Then, for a longitudinal polarization with $\vec{P}^{(2)}(\omega_p,\vec{k}_p)\|\vec{k}_p$, or for an homogenous polarization with $\vec{k}_p=0$,

$$E_i^P = -\frac{1}{\epsilon_0 \epsilon_{ii}} P_i^{(2)}, \tag{13}$$

while for a transverse polarization ($\vec{P}^{(2)} \perp \vec{k}_p$) the solution of the wave equation is

$$E_i^P = \frac{1}{\epsilon_0} \frac{P_i^{(2)}}{(k_p c/\omega_p)^2 - \epsilon_{ii}(\omega_p)}, \tag{14}$$

under the assumption that the wave vector mismatch between the nonlinear polarization and a propagating wave is so high that $\vec{E}^P$ has the same spatial and time dependence as the source polarization $\vec{P}^{(2)}$. As an example, for non-phase-matched frequency doubling of one field $\vec{E}=\vec{E}(\omega,\vec{k})$, $k_p=2k$, $\omega_p=2\omega$, and Eq. (14) becomes $E_i^P = (1/\epsilon_0)P_i^{(2)}/[\epsilon_{ii}(\omega)-\epsilon_{ii}(2\omega)]$, as was found, e.g., in Ref. [6].

For a static, plane-wave modulated nonlinear polarization, the solution of Eqs. (10) and (11) is [11,12]

$$\vec{E}^P(\vec{k}) = -\vec{k}\,\frac{k_j P_j^{NL}(\vec{k})}{\epsilon_0 k_k \epsilon_{kl} k_l}, \tag{15}$$

which reduces to Eq. (13) for a longitudinal polarization and to $\vec{E}^P=0$ for a transverse polarization. The electric field is in this case always parallel to the wave vector of the nonlinear polarization, reflecting the requirement that the curl of the electric field be zero.

From the above it is clear that the existence of an electric field associated to the nonlinear polarization, or its magnitude, depends on the circumstances. For the following discussion it is useful to write

$$E_i^P = \frac{1}{\epsilon_0}\zeta_{ij} P_j^{NL}, \tag{16}$$

where ζ_{ij} is defined by the expressions above. For any longitudinal polarization, $\zeta_{ii}=-1/\epsilon_{ii}$; for a transverse static polarization, $\zeta_{ii}=0$, while for a transverse, oscillating polarization ζ_{ii} has a pole at $(k_p c/\omega_p)^2=\epsilon_{ii}(\omega_p)$. The importance of these variations in ζ_{ij} will become evident when discussing DFWM later on.

Consider now how the polarization (9) can interact with the third optical wave $\vec{E}^3$ to generate a new nonlinear polarization $\vec{P}^{(C)}$, which is then of the third order in the fields $\vec{E}^1,\vec{E}^2,\vec{E}^3$. Evidently, when the polarization (9) generates a field $\vec{E}^P$ given by Eq. (16), second-order nonlinear optical interaction of $\vec{E}^P$ and $\vec{E}^3$ contributes a term

$$K_2 \epsilon_0 \chi_{ijq}^{(2)}(-\omega_c,\omega_3,\omega_p) E_j^3 E_q^P, \tag{17}$$

to the effective third-order polarization $P_i^{(C)}$. But this is not the only possibility. The nonlinear optical polarization can also combine directly with $\vec{E}^3$, even when $\vec{E}^P=0$ [6]. Calculating the magnitude of this direct contribution is nontrivial because the nonlinear optical susceptibilities are defined and measured using applied electric fields, not polarizations. One way to do this is to move to the microscopic level and consider the effects of the nonlinear polarization and the electric field on a single polarizable unit (a ''molecule'') in the material [6].

Denoting local fields and dipoles by lower case letters and, for the sake of simplicity, dropping temporarily the vector notation, we can write the local field induced by the nonlinear polarization $P^{(2)}$ as $e^P=LP^{(2)}$, while E^3 generates a local field $e^3=f_3E^3$. L and f_3 are local-field factors that assume the values $L=1/(3\epsilon_0)$ and $f_3=1+\chi(\omega_3)/3$ in the Lorentz local-field approximation [20]; $\chi(\omega_3)$ is the linear polarizability. The subscripts of the local-field factors f_i indicate the frequency at which they must be taken. By second-order nonlinear optics, the local fields e^P and e^3 generate a nonlinear dipole $p^C=K_2\epsilon_0\alpha^{(2)}e^Pe^3$, where $\alpha^{(2)}$ is the microscopic second-order susceptibility. To move back to the macroscopic level, the average macroscopic nonlinear polarization $P^{(C)}$ must be derived from the nonlinear dipole p^C using $P^C=Nf_cp^C$, and the macroscopic second-order susceptibility is related to $\alpha^{(2)}$ by $\chi^{(2)}(-\omega_1,\omega_2,\omega_3) = Nf_1f_2f_3\alpha^{(2)}(-\omega_1,\omega_2,\omega_3)$ [21]. Here, N is the number density of ''molecules.'' From this, one obtains $P^{(C)}$ as a function of the macroscopic quantities $P^{(2)}$, E^3, and $\chi^{(2)}$. Going back to vector notation, this direct contribution to $\vec{P}^{(C)}$ can be written as

$$K_2 \epsilon_0 \chi_{ijq}^{(2)}(-\omega_c,\omega_3,\omega_p) E_j^3 L \frac{\delta_{qp}}{f_p} P_p^{(2)}. \tag{18}$$

The final expression for the total cascaded polarization $\vec{P}^{(C)}$ is obtained by summing Eqs. (17) and (18),

$$P_i^{(C)} = K_2 \chi_{ijq}^{(2)}(-\omega_c,\omega_3,\omega_p) E_j^3 \left[\zeta_{qp} + \epsilon_0 L \frac{\delta_{qp}}{f_p}\right] P_p^{(2)}. \tag{19}$$

Substituting Eq. (9) for $\vec{P}^{(2)}$ and comparing the result with the form $P_i^{(C)}=K_3\chi_{ijkl}^{(C)}(-\omega_c,\omega_3,\omega_2,\omega_1)E_j^3E_k^2E_l^1$ for a third-order effect, one finds the following expression for the effective third-order susceptibility describing the cascaded contribution:

$$\begin{aligned}\chi_{ijkl}^{(C)}&(-\omega_c,\omega_3,\omega_2,\omega_1) \\ &= \frac{K_1K_2}{K_3}\chi_{ijq}^{(2)}(-\omega_c,\omega_3,\omega_p)\left[\zeta_{qp} + \frac{\epsilon_0 L\,\delta_{qp}}{f_p}\right] \\ &\quad \times \chi_{pkl}^{(2)}(-\omega_p,\omega_2,\omega_1).\end{aligned} \tag{20}$$

This is the final result of this section. It is valid in general for any two second-order processes that combine to contribute to a third-order process. A very important fact that is peculiar to this cascading process is that the ζ_{qp} term inside

the square brackets depends on the characteristics of the intermediate second-order polarization (9). The magnitude of the elements of the effective third-order susceptibility tensor describing the cascading effect will, therefore, change depending on the wave vector, frequency, and orientation of the intermediate second-order polarization, which are in turn influenced by details of the experimental geometry used. This is particularly true for the case of DFWM, because static and frequency-modulated second-order polarizations can both contribute to the signal at the same time.

III. CASCADED SECOND-ORDER EFFECTS IN DFWM

For noncentrosymmetric crystals, second-order nonlinear optical effects such as second-harmonic generation (SHG) and optical rectification (OR) become possible. Any two of the interacting beams in DFWM can give rise to a nonlinear optical polarization that can then interact with the third beam to produce the signal wave.

Referring to Fig. 1 for the labeling of the interacting fields, there are three second-order nonlinear-polarization components that play a role in the generation of the signal wave by cascaded second-order effects in DFWM [their wave vectors are found by picking any two terms, including their signs, from the sum $\vec{k}_1+\vec{k}_2-\vec{k}_3$ found in Eq. (3)].

The first one is produced by second-harmonic generation between wave 1 and wave 2. Its complex amplitude is

$$P_p^{(SH)}(2\omega,\vec{k}^{SH})=\epsilon_0\chi_{pkl}^{(2)}(-2\omega,\omega,\omega,-\vec{k}^{SH},\vec{k}_2,\vec{k}_1)\times E_k(\omega,\vec{k}_2)E_l(\omega,\vec{k}_1), \tag{21}$$

where $\vec{k}^{SH}=\vec{k}_1+\vec{k}_2$. It is interesting to note that for the phase-conjugation DFWM configuration of Fig. 1(b), $\vec{k}_1=-\vec{k}_2$, and $\vec{k}^{SH}=0$. The resulting wave vector of the ''second-harmonic'' polarization (21) is zero: it is a homogenous polarization density oscillating at the frequency 2ω that cannot radiate any electromagnetic wave, but which can still contribute to the DFWM signal.

The second one is produced by optical rectification between wave 1 and wave 3 and is

$$P_p^{(OR)}(\omega=0,\vec{k}_a^{OR})=\epsilon_0\chi_{pjl}^{(2)}(0,-\omega,\omega,-\vec{k}_a^{OR},-\vec{k}_3,\vec{k}_1)\times E_j(-\omega,-\vec{k}_3)E_l(\omega,\vec{k}_1), \tag{22}$$

with $\vec{k}_a^{OR}=\vec{k}_1-\vec{k}_3$.

The third one is produced by optical rectification between wave 2 and wave 3 and is

$$P_p^{(OR)}(\omega=0,\vec{k}_b^{OR})=\epsilon_0\chi_{pjk}^{(2)}(0,-\omega,\omega,-\vec{k}_b^{OR},-\vec{k}_3,\vec{k}_2)\times E_j(-\omega,-\vec{k}_3)E_k(\omega,\vec{k}_2), \tag{23}$$

with $\vec{k}_b^{OR}=\vec{k}_2-\vec{k}_3$.

A polarization of exactly the same form as Eq. (3), with frequency ω and wave vector $\vec{k}_4=\vec{k}_1+\vec{k}_2-\vec{k}_3$, is obtained when any of the above second-order polarizations—produced by a selected pair of input waves—combine with the remaining input wave. The corresponding ''cascaded'' mechanisms are (A) noncollinear second-harmonic generation through interaction of beams 1 and 2, and difference frequency generation between the polarization (21) generated in such a way and beam 3; and (B) optical rectification through interaction of beams 1 (or 2) and 3, and electro-optic interaction between the polarization (22) [or (23)] generated in such a way and beam 2 (or 1).

In the following, I will designate the effective third-order polarizations and susceptibilities induced by such ''cascaded'' processes as ''$\vec{P}^{(C,\vec{k})}$'' and ''$\chi^{(C,\vec{k})}$,'' where $\vec{k}$ identifies the wave vector of the relevant second-order polarization, e.g., $\vec{k}^{SH}$ when cascading occurs through the second-harmonic polarization (21). The genuine third-order polarization $P^{(3)}$ as well as any of the $\vec{P}^{(C,\vec{k})}$ radiate in a phase-matched way a wave that contributes to the total DFWM signal.

The effective third-order susceptibilities for the three cascaded processes introduced above are derived in the next sections.

A. Second-Harmonic Generation and Difference Frequency Generation

The interaction of the second-harmonic polarization (21) with the electric field $\vec{E}(\omega,\vec{k}_3)$ of the third ''input'' wave leads to an effective third-order polarization $P^{(C,\vec{k}^{SH})}$, which can be calculated using Eq. (19). In a coordinate system where the dielectric tensor is diagonal,

$$P_i^{(C,\vec{k}^{SH})}(\omega,\vec{k}_4)=\chi_{ijq}^{(2)}(-\omega,-\omega,2\omega,-\vec{k}_4,-\vec{k}_3,\vec{k}^{SH})\times E_j(-\omega,-\vec{k}_3)\left[\zeta_{qp}(\vec{k}^{SH})+\frac{\epsilon_0\delta_{qp}L}{f_p}\right]P_p^{(SH)}. \tag{24}$$

The local field factor f_p applies to the intermediate polarization (21) with a frequency of 2ω and polarized along p. The tensor $\zeta_{qp}(\vec{k}^{SH})$ is defined by Eqs. (13)–(14) and Eq. (16), and takes into account the macroscopic electric field that can be induced by the polarization $\vec{P}^{SH}(\vec{k}^{SH})$, as discussed in the previous section. Note that $\zeta_{qp}(\vec{k}^{SH})$ also depends on the frequency and on the direction of the intermediate polarization (21).

Inserting Eq. (21) into Eq. (24) one obtains

$$P_i^{(C,\vec{k}^{SH})}(\omega,\vec{k}_4)=\epsilon_0\chi_{pkl}^{(2)}(-2\omega,\omega,\omega,-\vec{k}^{SH},\vec{k}_2,\vec{k}_1)\times\chi_{ijq}^{(2)}(-\omega,-\omega,2\omega,-\vec{k}_4,-\vec{k}_3,\vec{k}^{SH})\times E_j(-\omega,-\vec{k}_3)E_k(\omega,\vec{k}_2)E_l(\omega,\vec{k}_1)\times\left[\zeta_{qp}(\vec{k}^{SH})+\frac{\delta_{qp}}{n_p^2+2}\right], \tag{25}$$

where we introduced the Lorentz expressions for f_p and L, and we used the refractive index $n_p^2=\epsilon_{pp}(2\omega)$.

In Eq. (25), the second-order susceptibilities describe second-harmonic and difference-frequency generation. They can both be expressed in terms of the frequently used d_{ijk} coefficients

$$\chi^{(2)}_{pkl}(-2\omega,\omega,\omega,-\vec{k}^{SH},\vec{k}_2,\vec{k}_1)=2d_{pkl}, \tag{26}$$

$$\chi^{(2)}_{ijq}(-\omega,-\omega,2\omega,-\vec{k}_4,-\vec{k}_3,\vec{k}^{SH})=2d_{qij}, \tag{27}$$

where the factor of 2 has no special significance and only reflects how the ''d coefficients'' were originally defined.

Following the same way used to derive the general expression (20), Eq. (25) can be compared to Eq. (3) to obtain the effective third optical susceptibility for the SHG/DFG contribution

$$\chi^{(C,\vec{k}^{SH})}_{ijkl}=\frac{8d_{qij}d_{pkl}}{3}\left[\zeta_{qp}(\vec{k}^{SH})+\frac{\delta_{qp}}{n^2_{pp}+2}\right], \tag{28}$$

where a factor of 2/3 had to be introduced because of the degeneracy factor in Eq. (3), and a factor of 4 comes from the definition of the d coefficients.

As discussed before, $\zeta_{qp}(\vec{k}^{SH})$ assumes different values depending on the characteristics of the second-harmonic polarization. For the phase-conjugation DFWM configuration of Fig. 1(b), and whenever the second-harmonic polarization is longitudinal, $\zeta_{qp}(\vec{k}^{SH})=-\delta_{qp}/\epsilon_{pp}$ as found in Eq. (13), and Eq. (28) becomes

$$\chi^{(C,\vec{k}^{SH})}_{ijkl}=-\frac{8d_{pij}d_{pkl}}{3}\frac{2}{n^2_{pp}(n^2_{pp}+2)}. \tag{29}$$

For a transverse second-harmonic polarization, a situation that can only arise in the forward DFWM configuration of Fig. 1(a), $\zeta_{qp}=\delta_{qp}\{[kc/(2\omega)]^2-n^2_{pp}(2\omega)\}^{-1}$ as found in Eq. (14). Then Eq. (28) becomes

$$\chi^{(C,\vec{k}^{SH})}_{ijkl}=\frac{8d_{pij}d_{pkl}}{3}\left[\frac{1}{[k^{SH}c/(2\omega)]^2-n^2_{pp}(2\omega)}+\frac{1}{n^2_{pp}(2\omega)+2}\right]. \tag{30}$$

The completely different role played by the SHG/DFG process for DFWM in the two possible experimental geometries is immediately visible from Eqs. (29) and (30). While for the phase-conjugation geometry the SHG/DFG contribution is always independent of the wave vectors of the interacting beams, for the forward geometry the SHG/DFG contribution becomes very sensitive on the birefringence of the material and on the orientation of the wave vector of the intermediate second-harmonic polarization (this wave vector vanishes for the phase-conjugation DFWM configuration).

For the phase-conjugation DFWM setup of Fig. 1(b), Eq. (29) always applies. In this case the second-harmonic polarization is spatially homogenous and $\chi^{(C,\vec{k}^{SH})}_{ijkl}$ is a constant, only dependent on the polarizations of the interacting beams, in the same way as $\chi^{(3)}_{ijkl}$. This is an important point because it means that in this configuration the SHG/DFG cascading contribution cannot be distinguished from the direct third-order contribution. It would, therefore, be possible, in principle, to include the SHG/DFG contribution in the numerical value of $\chi^{(3)}_{ijkl}$. This will not be the case for the OR/EO contribution, or for the SHG/DFG contribution in the forward DFWM setup of Fig. 1(a).

The SHG/DFG contribution for the phase-conjugation DFWM geometry is normally relatively modest. An order-of-magnitude evaluation of Eq. (29) using a refractive index of ~ 2 gives $\chi^{(C,\vec{k}^{SH})}_{ijkl}\sim -0.2d_{pij}d_{pkl}$, which for $d_{pij}=d_{pkl}=10$ pm/V becomes $\chi^{(C,\vec{k}^{SH})}_{ijkl}\sim 0.2\times 10^{-22}$ m^2/V^2, more than an order of magnitude less than the third-order susceptibility of fused silica, which is $\chi^{(3)}_{1111}=4\times 10^{-15}$ esu$=2\times 10^{-22}$ m^2/V^2 [18,22–24]. In this example we used susceptibility values that are typical of inorganic materials, and the relatively low contribution of the SHG/DFG process can also be understood on the basis of the frequency dependence of the material excitations that contribute to the various processes: while the contribution of ionic motion (optical phonons) to DFWM is allowed and large, only the electronic response contributes to frequency doubling [9]. For organic materials, on the other hand, the nonlinearity is given by the response of the electron clouds for practically all frequency combinations, which should tend to make the SHG/DFG contribution more comparable to the direct third-order contribution. More detailed examples of the magnitude of the SHG/DFG contributions for different materials and experimental geometries will be given later on.

The magnitude of the SHG/DFG contribution to DFWM in the phase-conjugation experimental geometry has also been calculated in Ref. [11]. But there the direct contribution of the nonlinear polarization [the term proportional to $1/(n^2+2)$ in (28)] was not taken into account. As a consequence, the treatment of the SHG/DFG contribution given in Ref. [11] predicts effective third-order susceptibilities with the wrong sign, and which are too large by a factor $(n^2+2)/2$. This lead to effective third-order susceptibilities substantially larger than the ones given here.

The cascaded contribution by SHG/DFG in the forward DFWM setup of Fig. 1(a) is also given by Eq. (29) whenever the second harmonic polarization is longitudinal. For a transverse polarization, however, the effective susceptibility is given by Eq. (30) and it depends on the refractive index dispersion. In Eq. (30) one recognizes the possibility that the second-harmonic polarization radiates a wave, because it has a pole for $k^{SH}=2\omega n_{pp}/c$. Obviously, the fact that Eq. (30) diverges when the second harmonic polarization is phase matched to a propagating electromagnetic wave of the same frequency and wave vector requires a different solution that takes into account the linear growth of the radiated wave with propagation distance. However, this phase-matching condition will be very sensitive to the intersection angle and the polarization of the interacting beams. It would be easily detected experimentally and should not adversely affect DFWM experiments as long as one avoids the particular beam crossing angles, if they exist, where the phase-

matching condition is satisfied. In the following we consider only the SHG/DFG contributions that always contributes to DFWM, independent of phase-matching conditions for SHG.

The magnitude and characteristics of the SHG/DFG contribution in the forward DFWM geometry can be better understood by considering the limit of a small angle β (outside the sample) between beams 1 and 2. Then one can write $k^{SH}=|\vec{k}_1+\vec{k}_2|=\cos(\beta/2)[n_k(\omega)+n_l(\omega)]\omega/c$, and

$$\chi_{ijkl}^{(C,\vec{k}^{SH})}=\frac{8d_{pij}d_{pkl}}{3}\left[\frac{1}{([n_k(\omega)+n_l(\omega)]/2)^2-n_{pp}^2(2\omega)}+\frac{1}{n_{pp}^2(2\omega)+2}\right]. \tag{31}$$

is a good approximation for Eq. (30). Consider for example $\chi_{1111}^{(C,\vec{k}^{SH})}$. Since $n_1(\omega)<n_1(2\omega)$ because of dispersion, the first term in the square brackets is negative. And since it has a difference of refractive indices in the denominator it dominates over the second term. One sees that the SHG/DFG contribution has the potential of becoming large and negative for diagonal elements of $\chi_{ijkl}^{(C,\vec{k}^{SH})}$ and for materials with low dispersion, while it also depends on the birefringence for nondiagonal elements of the susceptibility tensor. Some examples for specific inorganic and organic materials will be given below.

As a final comment to conclude this section it is interesting to note that it would be wrong to expect that SHG/DFG does not contribute to DFWM because the SHG process is not phase matched. After the two-step SHG/DFG process takes place, the resulting effective third-order polarization (25) is perfectly phase matched to the direct third-order polarization (3) (the signals radiated by both polarizations are in phase). Thus the contribution of SHG/DFG is *always* phase matched for DFWM. The fact that the SHG process itself is not phase matched only affects the magnitude of the effective third-order susceptibility (28) by influencing the value of $\zeta_{qp}(\vec{k}^{SH})$ when $\vec{P}^{(C,\vec{k}^{SH})}$ is transverse.

B. Optical rectification and Pockels effect

The effective third-order polarizations $P^{(C,\vec{k}_a^{OR})}$ and $P^{(C,\vec{k}_b^{OR})}$ induced by OR/EO cascading can be calculated using (19)

$$P_i^{(C,\vec{k}_a^{OR})}(\omega,\vec{k}_4)=\chi_{iqk}^{(2)}(-\omega,0,\omega,-\vec{k}_4,\vec{k}_a^{OR},\vec{k}_2)\times\left[\zeta_{qp}(\vec{k}_a^{OR})+\frac{\delta_{qp}}{\epsilon_{pp}+2}\right]P_p^{OR}(\vec{k}_a^{OR})\times E_k(\omega,\vec{k}_2), \tag{32}$$

$$P_i^{(C,\vec{k}_b^{OR})}(\omega,\vec{k}_4)=\chi_{iql}^{(2)}(-\omega,0,\omega,-\vec{k}_4,\vec{k}_b^{OR},\vec{k}_1)\times\left[\zeta_{qp}(\vec{k}_b^{OR})+\frac{\delta_{qp}}{\epsilon_{pp}+2}\right]P_p^{OR}(\vec{k}_b^{OR})\times E_l(\omega,\vec{k}_1), \tag{33}$$

where $\vec{k}_4=\vec{k}_a^{OR}+\vec{k}_2=\vec{k}_b^{OR}+\vec{k}_1$ and the Lorentz value for L/f_p was used. Because the polarizations (22) and (23) are static, the (diagonal) dielectric tensor must be taken at a frequency defined by the length of the optical pulses, while $\zeta_{qp}(\vec{k}_a^{OR})$ and $\zeta_{qp}(\vec{k}_b^{OR})$ are given by Eq. (15).

Inserting Eqs. (22)–(23) into Eqs. (32)–(33) one obtains the third-order polarizations induced by the two step process of optical rectification and Pockels effect. Once again, they have exactly the same form as Eq. (3), with frequency ω and wave vector $\vec{k}_4$,

$$P_i^{(C,\vec{k}_a^{OR})}(\omega,\vec{k}_4)=\epsilon_0\chi_{iqk}^{(2)}(-\omega,0,\omega,-\vec{k}_4,\vec{k}_a^{OR},\vec{k}_2)\times\chi_{pjl}^{(2)}(0,-\omega,\omega,-\vec{k}_a^{OR},-\vec{k}_3,\vec{k}_1)\times\left[\zeta_{qp}(\vec{k}_a^{OR})+\frac{\delta_{qp}}{\epsilon_{pp}+2}\right]\times E_j(-\omega,-\vec{k}_3)E_k(\omega,\vec{k}_2)E_l(\omega,\vec{k}_1), \tag{34}$$

$$P_i^{(C,\vec{k}_b^{OR})}(\omega,\vec{k}_4)=\epsilon_0\chi_{iql}^{(2)}(-\omega,0,\omega,-\vec{k}_4,\vec{k}_b^{OR},\vec{k}_1)\times\chi_{pjk}^{(2)}(0,-\omega,\omega,-\vec{k}_b^{OR},-\vec{k}_3,\vec{k}_2)\times\left[\zeta_{qp}(\vec{k}_b^{OR})+\frac{\delta_{qp}}{\epsilon_{pp}+2}\right]\times E_j(-\omega,-\vec{k}_3)E_k(\omega,\vec{k}_2)E_l(\omega,\vec{k}_1). \tag{35}$$

It is interesting to discuss the case of quasi-degenerate four-wave mixing, described by a third-order susceptibility of the kind $\chi_{ijkl}^{(3)}(-\omega_4,-\omega_3,\omega_2,\omega_1,-\vec{k}_4,-\vec{k}_3,\vec{k}_2,\vec{k}_1)$, where the difference between any of the ω_i is small compared to their value. In this case the OR/EO process goes over to a difference frequency generation plus Sum Frequency Generation process (DFG/SFG). The second-order susceptibilities $\chi_{iqk}^{(2)}$ and $\chi_{pjl}^{(2)}$ appearing in Eq. (34) must be replaced by $\chi_{iqk}^{(2)}(-\omega_4,\omega_a,\omega_2,-\vec{k}_4,\vec{k}_a^{DF},\vec{k}_2)$ and $\chi_{pjl}^{(2)}(-\omega_a,-\omega_3,\omega_1,-\vec{k}_a^{DF},-\vec{k}_3,\vec{k}_1)$ [and equivalently for Eq. (35)]. The polarization with wave vector $\vec{k}_a^{DF}$ is in this case a difference-frequency polarization oscillating at a small frequency. In principle, one should, therefore, use the ζ_{qp} derived from Eqs. (13) and (14) instead of Eq. (15) in the expressions (32) and (34). This affects the value of ζ_{qp} only in the case where the second-order polarization is transverse and Eq. (14) applies. However, even in this case one sees from Eq. (14) that ζ_{qp} tends to zero for a small frequency ω_p (corresponding to the present difference-frequency ω_a), so that one gets a smooth transition from the quasi-DFWM case to the DFWM case (remember that the wave vector $\vec{k}_p$, set by frequency and crossing angle of two input beams, is essentially independent from the difference-frequency ω_p). This shows that the present treatment also applies in the case of quasi-degenerate four-wave mixing. The expressions de-

rived here apply directly when the difference-frequencies ω_a and ω_b are small compared to the typical infrared resonance frequencies of a material, and will have to take into account the corresponding resonances otherwise.

The second-order susceptibilities appearing in Eqs. (34)–(35) are those that describe electro-optic effect and optical rectification. Permuting indices and frequency/wave vector arguments they can be expressed in terms of the standard electro-optic coefficients

$$\chi^{(2)}_{iqk}(-\omega,0,\omega,-\vec{k}_4,\vec{k}^{OR}_a,\vec{k}_2)=-\frac{1}{2}n_i^2n_k^2r_{ikq}, \tag{36}$$

$$\chi^{(2)}_{pjl}(0,-\omega,\omega,\vec{k}^{OR}_a,-\vec{k}_3,\vec{k}_1)=-\frac{1}{2}n_l^2n_j^2r_{jlp}. \tag{37}$$

Using these relations and comparing Eqs. (34)–(35) with Eq. (3) we find the equivalent of Eq. (20) for the present special case, that is, the effective third-order susceptibilities that describe the cascading processes related to the second-order polarizations with wave vectors $\vec{k}^{OR}_a$ and $\vec{k}^{OR}_b$ [13],

$$\chi^{(C,\vec{k}^{OR}_a)}_{ijkl}=\frac{1}{6}n_i^2n_j^2n_k^2n_l^2r_{ikq}r_{jlp}\left[\zeta_{qp}(\vec{k}^{OR}_a)+\frac{\delta_{qp}}{\epsilon_{pp}+2}\right], \tag{38}$$

$$\chi^{(C,\vec{k}^{OR}_b)}_{ijkl}=\frac{1}{6}n_i^2n_j^2n_k^2n_l^2r_{ilq}r_{jkp}\left[\zeta_{qp}(\vec{k}^{OR}_b)+\frac{\delta_{qp}}{\epsilon_{pp}+2}\right], \tag{39}$$

where $\zeta_{qp}(\vec{k}^{OR}_a)$ and $\zeta_{qp}(\vec{k}^{OR}_b)$ are given by

$$\zeta_{qp}(\vec{k})=-\frac{k_qk_p}{k_i\epsilon_{ij}k_j}. \tag{40}$$

The electro-optic coefficients and dielectric tensor used in Eqs. (38)–(39) are the strain-free values when the durations of the laser pulse used in a DFWM experiment is much shorter than the time needed by an acoustic wave to propagate over a distance given by the spatial period of the intermediate polarizations (22)–(23) [13,25]. The propagation time of a typical acoustic wave over a distance of 1 μm is generally of the order of a fraction of a nanosecond. When the modulation period of one of the intermediate polarizations (22)–(23) becomes very small [e.g., for Eq. (23) in the DFWM configuration of Fig. 1(b)], or for longer laser pulses, the electro-optic coefficients and dielectric constants to be used in Eqs. (38)–(39) must take into account the spatially modulated strain pattern that can form, and are given by [13,25]

$$r_{ijk}(\vec{k})=r^S_{ijk}+p_{ijmn}e_{klu}\hat{k}_n\hat{k}_u(A^{-1})_{ml}, \tag{41}$$

and

$$\epsilon_{ij}(\vec{k})=\epsilon^S_{ij}+\frac{1}{\epsilon_0}\hat{k}_n\hat{k}_ke_{imk}e_{jln}(A^{-1})_{ml}, \tag{42}$$

where $\vec{k}$ is the wave vector of the corresponding optically rectified polarization, r^S_{ijk} is the electro-optic tensor at constant strain, ϵ^S_{ij} is the dielectric tensor at constant strain, $\hat{k}_i=k_i/k$, p_{ijkl} is the elasto-optic tensor, e_{ijk} is the piezoelectric tensor, $A_{ik}=C^E_{ijkl}\hat{k}_j\hat{k}_l$, and C^E_{ijkl} is the elastic stiffness tensor.

As mentioned above, the effective third-order susceptibilities (38) and (39), calculated using the strain-free values of the electro-optic coefficients, are also valid for quasi-degenerate four-wave mixing as long as the frequency differences between the interacting beams are smaller than the typical optical phonon or vibronic frequencies of a material.

The two OR/EO contributions depend on the orientation of the intermediate polarizations (22)–(23) and of their wave vectors. This can be most easily seen by noticing how Eq. (40) is a projection operator that takes the component of the polarization which is parallel to its wave vector. Because of this effect, the OR/EO contribution will depend on the orientation of the sample for both DFWM geometries in Fig. 1, even when the directions of polarization of the interacting beams are kept constant inside the material. This allows the measurement of the OR/EO contributions by comparing the DFWM signal for different geometries [13]. The fact that a strain pattern can be established in the crystal on the picosecond and nanosecond time scale means that the OR/EO contribution will also depend on the magnitude of the wave vectors $\vec{k}^{OR}_a$ and $\vec{k}^{OR}_b$, not only on their direction [25]. This is particularly relevant when comparing experimental results obtained with the two different DFWM geometries in Fig. 1, because the spatial period corresponding to $\vec{k}^{OR}_b$ changes typically from a fraction of a micrometer for the setup in Fig. 1(b) to several micrometers for the setup in Fig. 1(a).

IV. EFFECTIVE THIRD-ORDER SUSCEPTIBILITY FOR DFWM

When the second-order processes outlined in the preceding section contribute to DFWM, the separate contributions from Eq. (28) and Eqs. (38)–(39) will add to the direct third-order susceptibility that must be used in Eq. (3). It makes, therefore, sense to define a total, effective, third-order susceptibility that takes into account all contributions to DFWM and that must replace $\chi^{(3)}_{ijkl}$ in Eq. (3) whenever a noncentrosymmetric material is used

$$\chi^{(3),\mathrm{EFF}}_{ijkl}=\chi^{(3)}_{ijkl}+\chi^{(C,\vec{k}^{SH})}_{ijkl}+\chi^{(C,\vec{k}^{OR}_a)}_{ijkl}+\chi^{(C,\vec{k}^{OR}_b)}_{ijkl}. \tag{43}$$

The $\chi^{(3),\mathrm{EFF}}_{ijkl}$ given here must be used in the standard expressions (3), (6), and (7) to calculate the effective third-order polarization and the corresponding DFWM signal [26].

In Eq. (43), $\chi^{(C,\vec{k}^{SH})}_{ijkl}$ is defined by Eq. (28) and can depend on magnitude and direction of the wave vector $\vec{k}^{SH}=\vec{k}_1+\vec{k}_2$ only for the forward-DFWM configuration [Fig. 1(a)]. $\chi^{(C,\vec{k}^{OR}_a)}_{ijkl}$ and $\chi^{(C,\vec{k}^{OR}_b)}_{ijkl}$ are defined by Eqs. (38)–(39), and always depend on the wave vector differences $\vec{k}^{OR}_a=\vec{k}_1-\vec{k}_3$ and $\vec{k}^{OR}_b=\vec{k}_2-\vec{k}_3$, in a manner described by the wave vector

dependent term $\zeta_{qp}(\vec{k})$ in Eqs. (38)–(39). $\chi^{(3)}_{ijkl}$, on the other hand, does not have any wave vector dependence under the assumption that the direct third-order interaction is a local process.

To analyze a DFWM experiment in a noncentrosymmetric material, it is important to be able to measure the direct third-order susceptibility $\chi^{(3)}_{ijkl}$, which is buried in the sum (43).

This could be done by determining $\chi^{(3),EFF}_{ijkl}$ with respect to a standard reference material, such as CS_2 or fused silica, and subtracting all the second-order contributions calculated for the experimental configuration that was used. This method relies both on the knowledge of the susceptibility of a reference material, and on the ability to predict the second-order contributions.

A better way is to exploit the geometry dependences of the second-order effects to measure their contribution to the signal, and use the calculated values of $\chi^{(C,\vec{k})}_{ijkl}$ to determine the absolute value of $\chi^{(3),EFF}_{ijkl}$, and, therefore, also of $\chi^{(3)}_{ijkl}$, without having to rely on a reference material [2,13].

Alternatively, using both a reference material and the knowledge about the geometry dependence of the second-order contributions, it is also possible to measure the magnitude of the second-order contributions with respect to the third-order susceptibility of the reference material. This could for example be used to determine the electro-optic coefficients in an all-optical way, and at frequencies of the order of the pulse length, e.g., of the order of 1 THz for 1 ps long pulses.

V. EXAMPLES OF THE EFFECT OF SECOND-ORDER CONTRIBUTIONS ON DFWM

The cascaded contributions (28), (38), and (39) assume considerably different values depending on experimental geometry and the material investigated. Since both the SHG/DFG contribution and the OR/EO contribution depend on boundary conditions, the effective values they assume depend both on DFWM configuration and on crystal orientation, not just on the polarization of the interacting beams. Some symmetry rules that are valid for direct third-order susceptibilities will not be valid anymore for the effective susceptibilities coming from a cascading of second-order contributions. This is clearly visible in the example of the OR/EO contributions alone, which can change a lot with sample orientation when the intermediate rectified polarizations change from transverse to longitudinal [13].

The difference in magnitude between the relative contributions of SHG/DFG cascading and of OR/EO cascading depends on the pulse length and material used, as well as on the experimental geometry. This is because optical phonons can contribute to genuine third-order DFWM and to OR/EO cascading, but not to SHG/DFG cascading. Thus, SHG/DFG cascading becomes comparable to the other effects in organic crystals or when using very fast laser pulses shorter than 100 fs, while its relative importance is generally smaller otherwise. However, SHG/DFG cascading can in all cases become considerably strong in the forward DFWM geometry [Fig. 1(a)], when the second-harmonic polarization is transverse.

TABLE I. Nonzero, strain-free electro-optic coefficients r^S_{ijk} (from Ref. [27]) and nonlinear optical coefficients d_{ijk} of $KNbO_3$ at a wavelength of 1.064 μm (taken from Ref. [28], and rescaled using $d_{111}=0.3$ pm/V for quartz). The dielectric constant (from Ref. [29]), and the refractive indices (from Ref. [30]) at the same wavelength $[n(\omega)]$ and at twice the frequency $[n(2\omega)]$ are also given.

ijk	r^S_{ijk} (pm/V)	d_{kij} (pm/V)	ϵ_{ii}	$n_i(\omega)$	$n_i(2\omega)$
333	30.5	20.5	37	2.1194	2.2031
223	64.0	13.7	780	2.2576	2.3814
113	16.0	11.8	24	2.2195	2.3226
232	348	12.8			
131	23.6	12.3			

These sometimes complicated dependencies of the cascaded contributions on several experimental details can be best clarified by giving examples of the corresponding effective third-order susceptibilities for various DFWM geometries and for a couple of different materials.

In the following I will give numerical values for the cascaded contributions from SHG/DFG and OR/EO for the two DFWM configurations in Fig. 1 and for two example materials: The organic salt DAST and the orthorhombic ferroelectric perovskite $KNbO_3$.

A. DFWM in the Inorganic Ferroelectric Crystal $KNbO_3$

$KNbO_3$ has point group mm2 with orthorhombic symmetry. As such, on a total of 81, it has 21 independent nonzero elements of the third-order susceptibility tensor. The additional symmetry introduced by frequency-degeneracy in DFWM means that, in our nomenclature, the first pair of indices and the last pair of indices are symmetric and separately interchangeable, so that the total number of independent elements of the direct third-order susceptibility tensor for DFWM reduces to 9: $\chi^{(3)}_{1111}$, $\chi^{(3)}_{2222}$, $\chi^{(3)}_{3333}$, $\chi^{(3)}_{1133}$ $\chi^{(3)}_{2233}$, $\chi^{(3)}_{1313}$, $\chi^{(3)}_{2323}$, $\chi^{(3)}_{1122}$, and $\chi^{(3)}_{1212}$.

Each index corresponds to a frequency and a wave vector parameter of $\chi^{(3)}_{ijkl}(-\omega,-\omega,\omega,\omega,-\vec{k}_4,-\vec{k}_3,\vec{k}_2,\vec{k}_1)$. In order to measure, e.g., $\chi^{(3)}_{1133}$ using any one of the DFWM setups in Fig. 1, beams 1 and 2 are polarized along 3, and beams 3 and 4 are polarized along 1. In order to simplify the discussion and the analysis, we assume a situation where the angles between the beams are small—so that light polarizations are well defined—and where the crystal faces are cut perpendicular to the crystallographic axes and are nearly perpendicular to the light beams.

The material properties of $KNbO_3$ that determine the magnitude of the cascaded contributions are given in Table I. The coordinate system used in $KNbO_3$ identifies the 3 axis with the polar c axis, so that the only nonzero second-order susceptibilities are the ones whose indices are any permutation of $ii3$, with $i=1,2,3$. The electro-optic coefficients are the strain-free ones that include optical-phonon contributions, so they are good for calculating the OR/EO contribu-

tions for DFWM with laser pulse durations of ~ 1 ps or longer.

To see see how the OR/EO and the SHG/DFG contributions arise from the data in Table I, consider again the example of $\chi^{(3)}_{1133}$. A rectified polarization with wave vector $\vec{k}_a^{OR}=\vec{k}_1-\vec{k}_3$ is induced by beams polarized along 3 and 1, respectively, via the electro-optic coefficient r_{131}. This rectified polarization is, therefore, polarized along 1, and it interacts with beam 2 (polarized along 3) via the electro-optic coefficient r_{131} to generate beam 4 (polarized along 1). The second-harmonic polarization has wave vector $\vec{k}^{SH}=\vec{k}_1+\vec{k}_2$ and it is induced by two beams polarized along 3, via the nonlinear optical coefficient d_{333}. The second-harmonic polarization is thus polarized along 3, and it interacts with beam 3 (polarized along 1) via the nonlinear optical coefficient d_{311} to generate beam 4 (polarized along 1). In the phase-conjugation DFWM setup $\vec{k}^{SH}=\vec{0}$ and the second-harmonic polarization is spatially homogenous and does not depend on the wave vectors of the interacting beams. This is not the case for the forward DFWM setup.

In order to show the various interplays between experimental geometry, sample orientation, OR/EO contribution, and SHG/DFG contribution, I calculate all contributions for both DFWM configurations in Fig. 1, two different orientations of the sample, and all third-order susceptibilities involving the indices 2 and 3. These susceptibilities can, e.g., be measured in a crystal with a polished face perpendicular to the 1 axis and beam wave vectors almost parallel to the 1 axis. These are also the tensor elements where the OR/EO contribution is largest, because of the large electro-optic tensor element r_{232} of $KNbO_3$. The results are displayed in Table II.

In Table II, the first column specifies the effective third-order susceptibility and, through its indices, the polarizations of the interacting beams in the sample reference frame. The column labeled *c* gives the orientation of the *c* axis of the crystal in the coordinate system defined in Fig. 1: *y* and *z* mean that the *c* axis is in the incidence plane of beams 1 and 3, or perpendicular to it, respectively (The SHG/DFG contribution is marked with "*y* and *z*" because it is the same for both sample orientations). The remaining columns list the second-order contributions for the two different DFWM geometries presented in Fig. 1. The two OR/EO contributions with different wave vectors are listed in separate columns, while the one SHG/DFG contribution is in a column by itself. For every contribution, the corresponding pair of electro-optic or nonlinear optical coefficients is also listed. The direct third-order contribution is the same for every horizontal section of Table II. Both $\chi^{(3)}_{3333}$ and $\chi^{(3)}_{2233}$ are of the order of $\sim 60\times 10^{-22}$ m^2/V^2 in $KNbO_3$ [13].

To give an example of its effect, I included piezoelectric elastic relaxation for the contribution with the large wave vector $\vec{k}_b^{OR}$ in Fig. 1(b) (phase-conjugation DFWM setup). For the large wave vector $\vec{k}_b^{OR}$ of the rectified polarization, the propagation velocity of elastic waves along $\vec{k}_b^{OR}$ can be so high that the crystal can elastically relax already during the light pulse. The OR/EO contributions for all other wave vectors have been calculated using the clamped (strain-free) coefficients, and are valid up to laser pulse lengths of several nanoseconds, depending on the angle between the beams. To obtain the effective susceptibility including elastic relaxation, I used the data in Ref. [29] to calculate the effective electro-optic tensor (41) and the effective dielectric tensor (42), and used the results in Eqs. (38)–(39). Without piezoelectric relaxation, $\chi^{(C,\vec{k}_b^{OR})}_{3333}=\chi^{(C,\vec{k}_a^{OR})}_{3333}=24\times 10^{-22}$ m^2/V^2 for the phase-conjugation setup and $c\|z$. For $\chi^{(3)}_{1133}$ and $\chi^{(3)}_{2233}$ the piezoelectric contribution for $\vec{k}_{a,b}\perp c$ always vanishes by symmetry, as can be demonstrated with Eq. (41). See Ref. [25] for further details on this effect.

It is important to note that the data in the table assumes that all light polarizations are kept constant in the sample reference frame when the sample orientation is changed from $c\|x$ to $c\|z$. While the direct third-order susceptibility does not change with crystal orientation or experimental setup, the indirect second-order contributions do. The considerable variations of the effective third-order susceptibilities listed in Table II obviously has important consequences for the interpretation of DFWM results in any centrosymmetric material.

TABLE II. Second-order cascaded contributions to DFWM in $KNbO_3$ for the two DFWM setups shown in Fig. 1. The contributions are listed separately for the two OR/EO contributions with wave vectors $\vec{k}_a^{OR}=\vec{k}_1-\vec{k}_3$ and $\vec{k}_b^{OR}=\vec{k}_2-\vec{k}_3$, and for the one SHG/DFG contribution with wave vector $\vec{k}^{SH}=\vec{k}_1+\vec{k}_2$. The effective third-order susceptibilities are given for two orientations of the crystal (*c*-axis parallel or perpendicular to the incidence plane defined by beams 1 and 3), and are in units of 10^{-22} m^2/V^2. The OR/EO contributions with wave vector $\vec{k}_b^{OR}$ for the case of Fig. 1(b) have been calculated taking into account elastic relaxation [25].

		Fig. 1(b)		Fig. 1(a)	
	c axis	$\vec{k}_a^{OR}$	$\vec{k}_b^{OR}$	$\vec{k}_a^{OR}$	$\vec{k}_b^{OR}$
$\chi^{(C,\vec{k})}_{3333}$		$r_{333}r_{333}$	$r_{333}r_{333}$	$r_{333}r_{333}$	$r_{333}r_{333}$
	y	-2	33	-2	24
	z	24	33	24	-2
$\chi^{(C,\vec{k}^{SH})}_{3333}$		$d_{333}d_{333}$		$d_{333}d_{333}$	
	y and *z*	-0.7		-29	
$\chi^{(C,\vec{k})}_{2233}=\chi^{(C,\vec{k})}_{3322}$		$r_{232}r_{232}$	$r_{232}r_{232}$	$r_{232}r_{232}$	$r_{232}r_{232}$
	y	136	136	136	-0.3
	z	-0.3	136	-0.3	136
$\chi^{(C,\vec{k}^{SH})}_{2233}$		$d_{333}d_{322}$		$d_{333}d_{322}$	
	y and *z*	-0.4		-20	
$\chi^{(C,\vec{k}^{SH})}_{3322}$		$d_{322}d_{333}$		$d_{322}d_{333}$	
	y and *z*	-0.4		32	
$\chi^{(C,\vec{k})}_{2323}$		$r_{333}r_{223}$	$r_{232}r_{232}$	$r_{333}r_{223}$	$r_{232}r_{232}$
	y	-5.5	136	-5.5	-3.5
	z	6.6	136	6.6	136
$\chi^{(C,\vec{k}^{SH})}_{2323}$		$d_{232}d_{232}$		$d_{232}d_{232}$	
	y and *z*	-0.2		-4.4	

As an example, the $\chi^{(3)}_{3333}$ coefficient can be measured with (i) $c\|y$ and all beams polarized along y, or (ii) $c\|z$ and all beams polarized along z. Depending on experimental configuration, several different results can be obtained. For the OR/EO contributions only r_{333} contributes to $\vec{P}^{OR}$, which is then parallel to c. For the phase-conjugation setup [Fig. 1(b)], both rectified polarizations are transverse for $c\|z$, while $\vec{P}^{OR}(\vec{k}_a^{OR})$ becomes longitudinal for $c\|y$. For the forward setup, $\vec{P}^{OR}(\vec{k}_a^{OR})$ is transverse and $\vec{P}^{OR}(\vec{k}_b^{OR})$ longitudinal for $c\|z$, and vice versa for $c\|y$. The total OR/EO contributions change by about a factor of two when rotating the sample (and all polarizations) by 90° in the phase-conjugation setup, or when switching to the forward DFWM geometry for a sample with the c axis parallel to z. The SHG/DFG contribution, on the other hand, is the same for both sample orientations but is very sensitive to the type of DFWM setup used, changing from being negligible in the phase-conjugation setup of Fig. 1(b) to being the dominant cascading contribution in the forward setup. Similar effects are observed for $\chi^{(3)}_{2233}$ and $\chi^{(3)}_{2323}$. Interestingly, in the forward setup, the *total* cascaded contribution does not depend on the orientation of the sample for all coefficients with the exception of $\chi^{(3)}_{2323}$.

The SHG/DFG contribution is negligibly small in all cases for the phase-conjugation DFWM configuration because in $KNbO_3$ the electronic response responsible for SHG/DFG is smaller than the optical-phonon contributions to EO/OR, and because the second-harmonic polarization is spatially homogenous. But the SHG/DFG contributions become important in the forward DFWM configuration of Fig. 1(a), where the second-harmonic polarization is a transverse plane wave, and the SHG process is nearer to phase matching.

It is very interesting to note that for the SHG/DFG contribution $\chi^{(3)}_{2233} \neq \chi^{(3)}_{3322}$, while for the direct third-order contribution and for the OR/EO contribution the symmetry rule $\chi^{(3)}_{ijmn} = \chi^{(3)}_{mnij}$ always applies. This can be explained as follows. For the SHG/DFG contribution to $\chi^{(3)}_{2233}$, the second-harmonic polarization is induced by beams polarized along 3, while for the SHG/DFG contribution to $\chi^{(3)}_{3322}$, the second-harmonic polarization is induced by beams polarized along 2. This does not matter for the DFWM configuration of Fig. 1(b), because there the electric field induced by the polarization does not depend on the refractive indices seen by the beams inducing the second-order polarization. But for the forward DFWM configuration the second-harmonic polarization is transverse. The magnitude of the electric field it generates depends on the phase mismatch between the beams inducing the second-harmonic polarization and a propagating wave at the second harmonic frequency. This destroys the $\chi^{(3)}_{2233} = \chi^{(3)}_{3322}$ symmetry. Moreover, normal refractive-index dispersion leads to a negative $\chi^{(C,\vec{k}^{SH})}_{2233}$, because here the polarizations of beams 1 and 2 and the second-harmonic polarization are parallel. $\chi^{(C,\vec{k}^{SH})}_{3322}$, on the other hand, is positive because here beams 1 and 2 have a polarization perpendicular to the second-harmonic polarization and the refractive index differences in the denominator of Eq. (30) change sign.

TABLE III. The largest electro-optic coefficients r_{ijk} (from Refs. [32,31]) and nonlinear optical coefficients d_{ijk} (from Ref. [33]) of DAST, at a wavelength of 1.54 μm. The dielectric constant (from Ref. [31]), and the refractive indices at the same wavelength $[n(\omega)]$ and at twice the frequency $[n(2\omega)]$ are also given.

ijk	r_{ijk} (pm/V)	d_{kij} (pm/V)	ϵ_{ii}	$n_i(\omega)$	$n_i(2\omega)$
111	47	290	6.5	2.13	2.40
221	21	41	2.5	1.60	1.69
331	<0.1		2.3	1.57	1.62
113	5				
212	14	39			

Table II is a good example of the sensitivity of the cascaded contributions to the choice of DFWM experimental setups and the sample orientation. The same kinds of geometry dependencies highlighted in Table II are expected in all noncentrosymmetric materials. Reference [13] presents some data on the OR/EO contributions to DFWM in tetragonal $BaTiO_3$, another ferroelectric perovskite. In $BaTiO_3$, the electro-optic coefficients are even larger than in $KNbO_3$, so that the importance of the OR/EO contributions is about twice as large as in $KNbO_3$.

From this example it is obvious that a correct inclusion of the second-order effects in DFWM measurements is of paramount importance for a correct reporting of experimental results, and in order to be able to compare experimental results obtained in different laboratories.

B. Cascaded Contributions to DFWM in the Organic Crystal DAST

To complete our practical examples of the second-order contributions to DFWM we consider an organic molecular crystal. We chose the organic salt DAST because it is one of the known organic crystals with better optical quality, high electro-optic and nonlinear optical susceptibilities, and is an ideal candidate for experiments. Moreover, it has high second- and third-order nonlinear optical response and some second-order contributions to DFWM have already been observed experimentally [31].

Table III gives the relevant material tensors of DAST, taken from the literature. Since DAST belongs to the point group m, it has ten independent second-order susceptibilities for OR/EO and SHG/DFG. The ones listed in the table are expected to be the largest ones because of the molecular orientation inside the DAST crystal [32,33], which makes the other coefficients negligible.

Similar to what was done for the example of $KNbO_3$, I calculate all second-order contributions for both DFWM configurations in Fig. 1, and two different orientations of the sample. For DAST, I calculate all third-order susceptibilities involving the indices 1 and 2, which can be measured in a crystal with a polished face perpendicular to the 3 axis and with beam wave vectors almost parallel to the 3 axis. The

TABLE IV. Second-order cascaded contributions to DFWM in DAST for the two DFWM setups shown in Fig. 1 and at a wavelength of 1.54 μm. The contributions are listed separately for the two OR/EO contributions with wave vectors $\vec{k}_a^{OR}$ and $\vec{k}_b^{OR}$, and for the one SHG/DFG contribution. The effective third-order susceptibilities are given for two orientations of the crystal (1-axis parallel or perpendicular to the incidence plane of beams 1 and 3), and are in units of 10^{-22} m^2/V^2.

		Fig. 1(b)		Fig. 1(a)	
	1 axis	$\vec{k}_a^{OR}$	$\vec{k}_b^{OR}$	$\vec{k}_a^{OR}$	$\vec{k}_b^{OR}$
$\chi_{1111}^{(C,\vec{k})}$		$r_{111}r_{111}$	$r_{111}r_{111}$	$r_{111}r_{111}$	$r_{111}r_{111}$
	y	183	183	183	-5.6
	z	-56	183	-5.6	183
		$r_{113}r_{113}$	$r_{113}r_{113}$	$r_{113}r_{113}$	$r_{113}r_{113}$
	y	4.1	-3.6	4.1	4.1
	z	4.1	-3.6	4.1	4.1
$\chi_{1111}^{(C,\vec{k}^{SH})}$		$d_{111}d_{111}$		$d_{111}d_{111}$	
	y and z	-100		-1545	
$\chi_{1122}^{(C,\vec{k})}=\chi_{2211}^{(C,\vec{k})}$		$r_{212}r_{212}$	$r_{212}r_{212}$	$r_{122}r_{122}$	$r_{212}r_{212}$
	y	-7.8	9.8	-7.8	9.8
	z	9.8	9.8	9.8	-7.8
$\chi_{1122}^{(C,\vec{k}^{SH})}$		$d_{122}d_{111}$		$d_{122}d_{111}$	
	y and z	-14		-218	
$\chi_{2211}^{(C,\vec{k}^{SH})}$		$d_{111}d_{122}$		$d_{111}d_{122}$	
	y and z	-14		-58	
$\chi_{1212}^{(C,\vec{k})}$		$r_{111}r_{221}$	$r_{212}r_{212}$	$r_{111}r_{221}$	$r_{212}r_{212}$
	y	26.1	9.8	29.8	-7.8
	z	-8.0	9.8	-8.0	9.8
$\chi_{1212}^{(C,\vec{k}^{SH})}$		$d_{212}d_{212}$		$d_{212}d_{212}$	
	y and z	-6		73.5	

long axis of the molecules in the DAST crystal is approximately oriented along the 1 axis, making the nonlinear optical contributions from this axis dominant over all others.

The results—obtained by using the data in Table III and Eqs. (28), (38), and (39)—are displayed in Table IV. As is readily visible from this table, the second-order contributions to DFWM in DAST have the same complicated geometry dependences as in $KNbO_3$, and the discussion of the preceding section applies also in this case, even though here the OR/EO contributions are less important when compared to the direct third order susceptibility. For DAST, $\chi_{1111}^{(3)}(-\omega, -\omega, \omega, \omega)$ is of the order of 3000×10^{-22} m^2/V^2 for ω corresponding to 1.064 μm (while $\chi_{1122}^{(3)}\sim500\times10^{-22}$ m^2/V^2) and $\chi_{1212}^{(3)}\sim300\times10^{-22}$ m^2/V^2) [31]. For the wavelength of 1.54 μm of interest here these values should probably be reduced by about 50%.

An important difference between this example of DAST and the previous example of $KNbO_3$, is that for DAST the SHG/DFG contributions are comparable to the OR/EO contributions also in the phase-conjugation DFWM configuration of Fig. 1(b) (while they were negligible in $KNbO_3$). In this organic crystal the electro-optic response as well as the frequency-doubling response both share a very large electronic contribution, while the optical-phonon contributions to OR/EO are relatively small. DFWM experiments at a wavelength of 1.06 μm in DAST, which demonstrated the presence of the OR/EO cascaded contributions have been reported in Ref. [31].

Also notable in Table IV is the very large SHG/DFG contribution to $\chi_{1111}^{(3)}$ in the forward DFWM configuration. This is caused by the fact that for this diagonal element the refractive index difference between a frequency ω and a frequency 2ω is only given by the refractive index dispersion between 1.5 μm and 0.7 μm, and not by the (relatively large) birefringence of DAST. Note also that $\chi_{1111}^{C,\vec{k}^{SH}}$ is large and negative, so that it tends to compensate the genuine third-order $\chi_{1111}^{(3)}$ in this configuration.

VI. CONCLUSIONS

This work presented a detailed discussion of all second-order contributions to degenerate four-wave mixing in noncentrosymmetric materials and gave general expressions for the corresponding effective third-order susceptibility that must be used to calculate the DFWM signal.

It was found that the three input beams in DFWM can combine pairwise to generate one second-harmonic polarization and two static-polarization gratings. The second-harmonic polarization is spatially homogenous in the phase-conjugation DFWM geometry, while it is modulated like a plane wave for the forward DFWM geometry. Everyone of the three second-order polarizations contributes to the DFWM signal, phase matched with each other and with the genuine third-order effect that is always present. For each second-order polarization, the magnitude of its contribution to the DFWM signal depends on the orientation of its spatial modulation.

Because of all these effects the effective susceptibility describing DFWM in noncentrosymmetric materials changes dramatically for different DFWM setups and on varying the orientation of the sample with respect to the wave vectors of the interacting beams, a fact that is very important when comparing third-order susceptibility values measured in different laboratories. Certain symmetry properties that are characteristic of the third-order susceptibility for DFWM in centrosymmetric materials do not exist anymore for DFWM in acentric materials. If properly taken into account, the dependence of the second-order contributions from sample orientation can be used to relate experimentally the values of third-order and second-order susceptibilities. This allows the measurement of the third-order susceptibility without relying on a reference material or on a detailed characterization of the spatial and temporal profile of the laser fields inside the sample.

To date, an experimental confirmation of the predictions of this work has been performed for the OR/EO contributions in the phase-conjugation DFWM geometry of Fig. 1(b) [13,31,25]. This gives support to the general theoretical approach used in this paper, and, therefore, also to the predic-

tions regarding the forward-DFWM setup of Fig. 1(a) and the SHG/DFG contributions.

DFWM is a standard tool for the determination of third-order susceptibilities. The theory and examples given in this work should help experimentalists towards a complete reporting of DFWM experiments, and towards a reliable determination of third-order susceptibilities of noncentrosymmetric materials by DFWM.

[1] T. K. Gustafson, J.-P. E. Taran, P. L. Kelley, and R. Y. Chiao, Opt. Commun. **2**, 17 (1970).

[2] E. Yablonovitch, C. Flytzanis, and N. Blomebergen, Phys. Rev. Lett. **29**, 865 (1972).

[3] S. D. Kramer, F. G. Parsons, and N. Bloembergen, Phys. Rev. B **9**, 1853 (1974).

[4] C. Flytzanis, in *Theory of Nonlinear Optical Susceptibilities*, Quantum Electronics Vol. 1, edited by H. Rabin and C. L. Tang (Academic Press, New York, 1975).

[5] S. D. Kramer and N. Bloembergen, Phys. Rev. B **14**, 4654 (1974).

[6] Chr. Flytzanis and N. Bloembergen, Prog. Quantum Electron. **4**, 271 (1977).

[7] H. J. Bakker, P. C. M. Planken, L. Kuipers, and A. Lagendijk, Phys. Rev. A **42**, 4085 (1990).

[8] R. DeSalvo, D. J. Hagan, M. Sheik-Bahae, G. Stegeman, and E. W. Van Stryland, Opt. Lett. **17**, 28 (1992).

[9] R. W. Hellwarth, Prog. Quantum Electron. **5**, 1 (1977).

[10] M. Zgonik and P. Günter, Ferroelectrics **126**, 33 (1992).

[11] P. Unsbo, J. Opt. Soc. Am. B **12**, 43 (1995).

[12] M. Zgonik and P. Günter, J. Opt. Soc. Am. B **13**, 570 (1996).

[13] I. Biaggio, Phys. Rev. Lett. **82**, 193 (1999).

[14] R. W. Hellwarth, J. Opt. Soc. Am. **67**, 1 (1977).

[15] P. D. Maker, R. W. Terhune, Phys. Rev. **137**, A801 (1964).

[16] P. N. Butcher and D. Cotter, *The Elements of Nonlinear Optics* (Cambridge University Press, Cambridge, England, 1991).

[17] This statement is also true for very short pulses in the forward setup of Fig. 1(a), but it only holds for pulse lengths longer than the material thickness for the phase-conjugation DFWM setup.

[18] F. P. Strohkendl, L. R. Dalton, R. W. Hellwarth, H. W. Sarkas, and Z. H. Kafafi, J. Opt. Soc. Am. B **14**, 92 (1997).

[19] Note that in Ref. [16] a degeneracy factor of 3/4 is listed for DFWM. This is an error.

[20] J. D. Jackson, *Classical Electrodynamics* (Wiley, New York, 1975).

[21] Y. R. Shen, *The Principles of Nonlinear Optics* (Wiley, New York, 1984).

[22] D. Milam, Appl. Opt. **37**, 546 (1998).

[23] U. Gubler and C. Bosshard, Phys. Rev. B **61**, 10 702 (2000).

[24] Note on units: The esu value given here follows the Maker and Terhune convention used in Ref. [18] and in a relevant part of the literature in esu. It must be multiplied by a factor of four to compare it to the esu values given in Ref. [23]. All fused-silica third order susceptibility values given in the three references agree to within 10%: Ref. [18] gives $4.06\pm0.05\times10^{-15}$ esu $=2.27\times10^{-22}$ m^2/V^2; from the nonlinear refractive index given in Ref. [22] one derives 2.2×10^{-22} m^2/V^2, while the newest third-harmonic-generation measurements of Ref. [23] lead to 2.0×10^{-22} m^2/V^2.

[25] I. Biaggio, Appl. Phys. Lett. **78**, 1861 (2001).

[26] This way of defining the effective susceptibility is at odds with what was done in Ref. [12], where the numerical factor of 3/2 present in the expression (3) was included in the value of the effective susceptibility. This definition did not allow a direct comparison of the numerical values of the genuine third-order susceptibility and the effective one.

[27] P. Bernasconi, M. Zgonik, and P. Günter, J. Appl. Phys. **78**, 2651 (1995).

[28] I. Biaggio, P. Kerkoc, L.-S. Wu, and P. Günter, J. Opt. Soc. Am. B **8**, 507 (1992).

[29] M. Zgonik, P. Bernasconi, M. Duelli, R. Schlesser, P. Günter, M. H. Garrett, D. Rytz, Y. Zhu, and X. Wu, Phys. Rev. B **50**, 5941 (1994).

[30] B. Zysset, I. Biaggio, and P. Günter, J. Opt. Soc. Am. B **9**, 380 (1992).

[31] Ch. Bosshard, I. Biaggio, St. Fischer, S. Follonier, and P. Günter, Opt. Lett. **24**, 196 (1999).

[32] F. Pan, G. Knöpfle, Ch. Bosshard, S. Follonier, R. Spreiter, M. S. Wong, and P. Günter, Appl. Phys. Lett. **69**, 13 (1996).

[33] U. Meier, M. Bösch, Ch. Bosshard, F. Pan, and P. Günter, J. Appl. Phys. **83**, 3486 (1998).